

# CYTOTOXIC AND GENOTOXIC EFFECT OF BIOFABRICATED ZINC NANOPARTICLES ON MITOTIC CHROMOSOMES OF *DRIMIA POLYANTHA* (ROXB.) JESSOP

Azharuddin Daphedar and Tarikere C Taranath\*

Environmental Biology Laboratory, P. G. Department of Studies in Botany,  
Karnataka University, Dharwad, Karnataka 580 003, India.

## ABSTRACT

Green synthesis of nanoparticles and their diverse applications are grown in various fields of nanoscience. In the present investigation, genotoxic effect of biogenic zinc nanoparticles on the root tip chromosomes of *Drimia polyantha* was evaluated. Biogenic zinc nanoparticles were characterized by UV-visible, XRD, FT-IR, AFM and HR-TEM analysis. The UV spectrum shows characteristic absorption peak at 374 nm. FTIR data suggested involvement of different functional groups in leaf extract were responsible for the reduction, capping and stabilization of ZnNPs. XRD results confirmed the crystalline nature of zinc nanoparticles with face centered cubic structure. AFM and HR-TEM images reveal the size and shape of nanoparticles. The size of ZnNPs ranges between 5 to 80 nm and are spherical in nature. The effect of zinc nanoparticles on mitotic index (MI) and the chromosomal aberrations (CAs) was determined by the exposing root meristematic cells of *D. polyantha* to different concentrations viz. 4, 8, 12 and 16 µg/ml of zinc nanoparticles suspension at the interval of 6, 12, 18 and 24 hrs. The investigation, revealed that the significant decrease ( $19.43 \pm 1.58$ ) in mitotic index and increase in chromosomal aberrations ( $36.09 \pm 3.29$ ), dose and duration dependent, when compared to control. The treated meristematic cells showed various types of chromosomal abnormalities including bridges, sticky, laggard, diagonal, C-metaphase, multipolar anaphase, disturbed metaphase and micronucleus.

## INTRODUCTION

Nanotechnology emerges from the physical, chemical, biological and engineering sciences where new techniques are being developed from single atoms and molecules for multiple applications in different field of science and technology. Among other metal nanoparticles zinc have received special focus in view of their distinctive, fascinating and extensive properties like semiconductor, chemical stability, catalytic, piezoelectric, and ultraviolet (UV)-shielding<sup>1-2</sup>. The researchers have attempted to synthesize nanoparticles within the size ranges between 1-100 nm. Moreover, the bio-nanotechnology exists, from a new branch of nanotechnology, which integrates principles of biology with physical and chemical procedures to generate tiny-sized particles with specific functions<sup>3-6</sup>. The physico-chemical based protocols for the synthesis of metallic nanoparticles are often expensive, toxic and utilize lethal chemicals. Bio-

based nanoparticles are relatively new and largely explored in the area of research. The "green" route for nanoparticle synthesis makes use of environmental friendly, non-toxic and safe reagents. As compared to physico-chemical synthesis, biological synthesis of nanoparticles are environmentally benign and economically green as they are simple, inexpensive and easily scale up larger scale production<sup>7-9</sup>. Recently, the bio-fabrication of zinc nanoparticles synthesized by leaf extracts of *Justica adathoda*<sup>10</sup>, *Limonia acidissima* leaf mediated synthesis of zinc oxide nanoparticles<sup>11</sup> and Biosynthesis of silver nanoparticles by leaf extract of *Albizia saman*<sup>12</sup> has been well documented.

Recently, there are few reports on phytotoxicity of ZnO nanoparticles on *Arabidopsis* and Rye grass (*Lolium perenne*) roots shows morphological changes at high concentration of ZnO nanoparticle, leads to shrinkage of root tips due to plasmolysis and contraction of epidermal

and cortical cells<sup>13-15</sup> noticed that zinc oxide nanoparticles inhibit the growth of bacterial cells due to the release of zinc ions from zinc nanoparticles, and induced toxicity via reactive oxygen species (ROS) involving hydrogen peroxide which lead to DNA damage<sup>16</sup>. Ahmed et al.,<sup>17</sup> reported that ZnO-NPs treated *Allium cepa* roots induce cytotoxicity and oxidative DNA damage during mitotic cell division with Zn<sup>2+</sup> ions in plants.

*Getonia floribunda* (Roxb.) belongs to family Combertaceae commonly known as life saver by the forest dwellers. The various parts of the plant are used to treat various ailments such as intestinal worms, colic, leprosy, malarial fever, dysentery, ulcers and vomiting<sup>18</sup>. Moreover, it possesses antibacterial activity, anticancer and antioxidant property<sup>19-20</sup>. In the present investigation, we have reported the biosynthesis and characterization of zinc nanoparticles using leaf extract of *G. floribunda* and their potential toxicity to mitotic cell division of *D. polyantha* (Blatt. & McCann) Stearn. family Asparagaceae. The effect of zinc nanoparticles on organism and environment are in nascent stage yet to be explored on different dimensions of their toxicity. However, there is no systematic work on this important aspect. Therefore, evaluation of the toxicological effects of nanoparticles on plants and their mitotic activity is essential. Hence the present investigation is carried out on cytotoxic/genotoxic impacts of zinc nanoparticles on *D. polyantha*.

## MATERIALS AND METHODS

### Plant materials

All chemicals used in the present study are obtained from spectrochem Pvt Ltd. and S. D. Fine-Chem Ltd, (Mumbai, India). The plant *Getonia floribunda* (synonym *Calycopteris floribunda*) leaves (Fig. 1) were collected from the Botanical garden of Karnatak University campus, Dharwad, Karnataka, India.

### Preparation of leaf extract

About 20 g fresh leaves were thoroughly washed in running tap water followed by double distilled water to remove adhered dust impurities. Washed leaves were shade dried, chopped into small pieces and added to 100 ml of Milli-Q water taken in 250 ml of Erlenmeyer flask and kept in water bath at 60°C for 1 hrs. The extract was filtered through Whatman filter paper No. 1. The filtrate was stored in refrigerator at 4°C for further experimental analysis.

### Phytosynthesis of zinc nanoparticles

The 1mM fresh silver nitrate (AgNO<sub>3</sub>) solution was prepared and 10 ml of *G. floribunda* leaf extract was added to 90 ml of 1mM silver nitrate solution and incubated at 60°C for 1 hr. Further, the temperature of reaction mixture was brought to room temperature and pH was adjusted to (pH 8.0, pH 9.0 and pH 10.0), the color of the reaction mixture was changed from light yellow to deep yellow indicating the formation of zinc nanoparticles (Fig. 2).



Fig. 1: a) *G. floribunda* leaf  
b) Formation of ZnNPs

### Characterization of zinc nanoparticles

The biosynthesized zinc nanoparticles were analyzed by UV-Vis spectrophotometer (Jasco V-670 UV-Vis NIR spectrophotometer) operated wavelength ranges between 300-700 nm with resolution at 1nm. The biomolecules present in *G. floribunda* leaf extract and involved in bioreduction and capping of zinc nanoparticles were investigated by FTIR analysis. The reaction solution was centrifuged for 40 min at 3500-4000 rpm, to obtain pellet of zinc nanoparticles. Thereafter, purified suspension was freeze dried to obtain dry powder. The powder of ZnNPs mixed with potassium bromide (KBr) to obtain a pellet, the spectra was recorded in the range 400-4000 cm<sup>-1</sup>. The purified dried powder of ZnNPs was used for X-Ray diffractometer (XRD) analysis to confirm the crystalline nature of the particles. XRD was performed in the 2θ range of 30 to 80 degrees. Morphology, size and distribution of the nanoparticles were analyzed by using atomic force microscopy (AFM) and high resolution transmission electron microscope (HR-TEM) images.

### *Drimia polyantha* assay

Healthy and uniformly sized bulbs of *D. polyantha* (2n=20) were collected from Shivaji University campus, Kholapur, Maharashtra, India. After collection, the bulbs were cleaned 2-3 times with tap water followed by double distilled water. The outer dry scales were

removed cautiously from the bulbs, without destroying root primordia. The bulbs were soaked in glass coupling jar containing Milli-Q water for 48 h. at room temperature. When the newly emerged roots reached 3-4 cm in length, than they were transferred to new coupling jars contain different concentrations of zinc nanoparticles solution (4, 8, 12 and 16  $\mu\text{g/ml}$ ) and treated for 6, 12, 18 and 24 hrs. After treatment the roots were excised and immediately fixed in Carnoy's solution (3 parts ethyl alcohol and 1 part glacial acetic acid i.e. 3:1) for 24 h. Then the roots were transferred to 70% ethyl alcohol and stored in a refrigerator at 4° C for cytological studies.

### Squash preparation

Squashes were prepared as suggested by Sharma <sup>21</sup>, to evaluate the mitotic index (MI) and chromosomal aberrations (CAs). For examination the root tips were placed in a watch glass and added 9 drops of aceto-orcein and 1 drop of HCl and warmed over a low flame for 2-3 minutes using spirit lamp. These were kept in room temperature for 5-10 minutes. After staining, the meristematic region were placed on clean slide and squashed under a cover glass and 500 cells were scored from each slide making a total between 1800-2200 cells for each concentration and control under a bright field microscope at 40X magnification <sup>22-24</sup>. The mitotic index was calculated by using formula  $MI = \text{Number of dividing cells} / \text{total number of analyzed cells} \times 100$  and chromosomal aberrations were calculated  $CAs = \text{Number of abnormal cells} / \text{total no. of dividing cells} \times 100$ .

### Statistical analysis

The data were analyzed by using IBM, SPSS Statistical version 20 windows software followed by two-way ANOVA and Tukey test.

## RESULTS AND DISCUSSION

### UV-Vis spectroscopy

The UV-vis absorption spectrum was used to monitor the biosynthesis of zinc nanoparticles using *G. floribunda* leaf extract (Fig. 1). The addition of 10 ml leaf extract of *G. floribunda* was added to 90 ml of  $\text{ZnNO}_3$  solution in a 250 ml Erlenmeyer flask, the reaction mixture was incubated at 80° C for 10-15 minutes. The pH was adjusted to 8, 9 and 10 using either 0.1N HCl or 0.1 N NaOH. The changes in the color of the solution were due to reduction of  $\text{ZnNO}_3$  to ZnNPs, has a plasmon resonance peak at 374 nm at pH 8 are represented in Figure 1 and 2. But, In case of pH 9 and 10 the absorption peak observed at 381 and 386 nm, which shows

broad peaks as compared to pH-8. Our observation was similar to the synthesis of zinc oxide nanoparticles by *L. aculeata* leaf extract <sup>25</sup>.

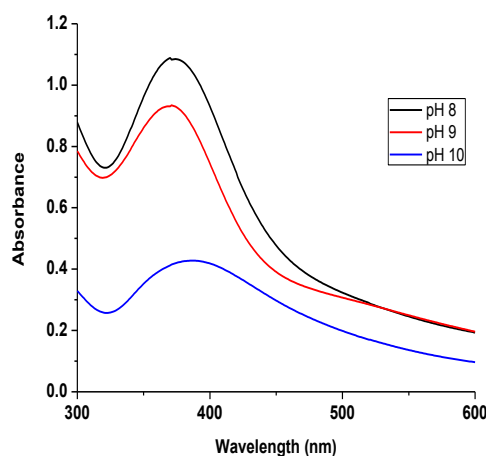


**Fig. 2: UV-Vis absorption spectrum of ZnNPs synthesized by leaf extract of *G. floribunda***

### FTIR analysis

FTIR spectra of the nanoparticles were recorded in order to identify the possible biomolecules involved in the reduction and capping/stabilization of the synthesized zinc nanoparticles. Figure-3 and Table-1 shows the FTIR spectra of ZnNPs. The spectrum of ZnNPs shows characteristic absorbance bands at 3438.72, 2923.69, 2854.15, 1740.87, 1629.73, 1458.85, 1113.80 and 1029.93  $\text{cm}^{-1}$ , whereas, IR bands of *G. floribunda* leaf extract were noticed at 3434.13, 2923.94, 2853.94, 1746.28, 1631.69, 1454.28, 1115.29 and 1058.39  $\text{cm}^{-1}$  respectively. A shift in the peak from 3434.13 to 3438.72  $\text{cm}^{-1}$  is due to the stretching of O-H and H-bending vibrations of alcohols and phenols. Shift was observed in the peak at 2923.94 to 2923.69  $\text{cm}^{-1}$  is because of O-H stretching of carboxylic acid <sup>26</sup>. A shift was observed from 2853.94 to 2854.15  $\text{cm}^{-1}$  is due to the asymmetric stretching of the C-H group. Another shift was observed from 1746.28 to 1740.87  $\text{cm}^{-1}$  is because of C=O stretching modes of the carbonyl functional group in ketones, aldehydes and carboxylic acids. The shift in absorption peak at 1631.69 to 1629.73  $\text{cm}^{-1}$  may be assigned to conjugation effect of N-H stretching <sup>27</sup>. The shift in the weak band 1115.29 to 1113.80  $\text{cm}^{-1}$  and 1058.39 to 1029.93  $\text{cm}^{-1}$  was due to the involvement of aromatic and aliphatic amines (C-N stretch) or C-O stretching vibrations of phenolic compounds.

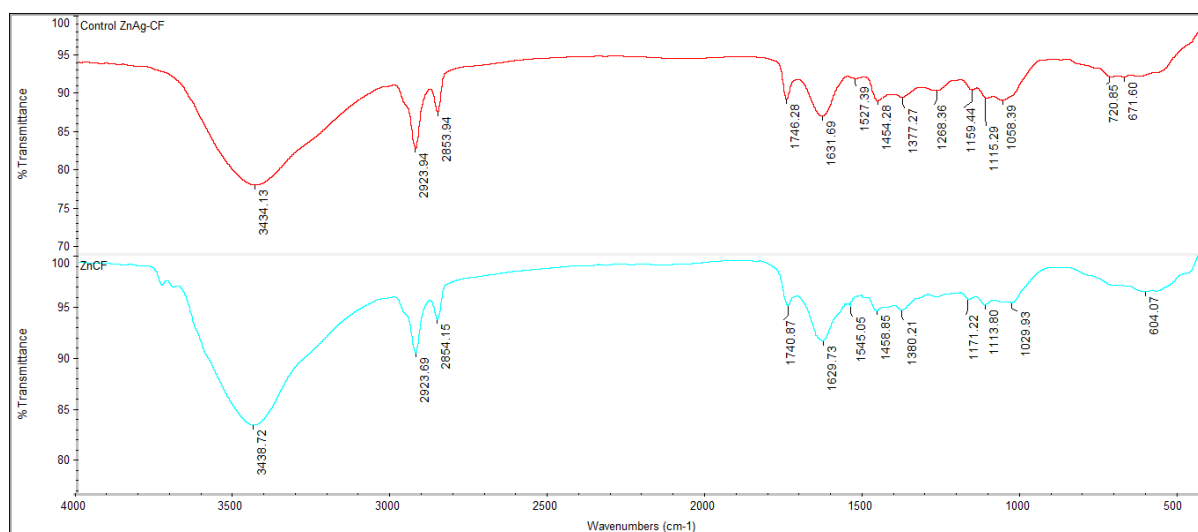


Fig. 3: FTIR spectra of ZnNPs synthesized by *G. floribunda* and leaf extract

Table 1: FTIR absorption peaks and their functional groups of ZnNPs synthesized by leaf extract of *G. floribunda*

Sl.No.	Absorption peak cm <sup>-1</sup> of leaf extract	Absorption peak cm <sup>-1</sup> of Silver nanoparticles	Functional groups
1	3434.13	3438.72	O-H stretch, H-bending vibrations of alcohols and phenols
2	2923.94	2923.69	O-H stretch Carboxylic acid, Alkyl C-H Stretch
3	2853.94	2854.15	Asymmetric stretching of the C-H group
4	1746.28	1740.87	C=O stretching modes of the carbonyl functional group in ketones, aldehydes and carboxylic acids
5	1631.69	1629.73	N-H stretching
6	1454.28	1458.85	C-H bond
7	1115.29	1113.80	Aromatic amines
8	1058.39	1029.93	Aliphatic amines (C-N stretch) or C-O stretching vibrations of phenolic compounds

### XRD analysis

X-ray diffraction (XRD) analysis of the ZnNPs synthesized by *G. floribunda* leaf extract has been carried out (Fig. 4). The presence of peaks located at  $2\theta$  angles corresponds to (111), (200), (220) and (311) shows high intense peak can be indexed as  $38.45^\circ$ ,  $44.12^\circ$ ,  $64.26^\circ$  and  $78.48^\circ$  planes of face cubic centered (fcc) of zinc, respectively (Figure-4). Thus, the XRD spectrum confirmed crystalline nature of ZnNPs. The average size of zinc nanoparticles can be calculated by using (111) Bragg's reflection  $D = K\lambda / \cos\theta$ . Where  $K$  is the Scherrer constant ( $K=0.94$ ),  $\lambda$  is the wavelength of the X-ray,  $\beta$  is the FWHM (full width and half maximum) of the peak and  $\theta$  is the half of the Bragg angle. The size of the nanoparticle found to be 40.15 nm.

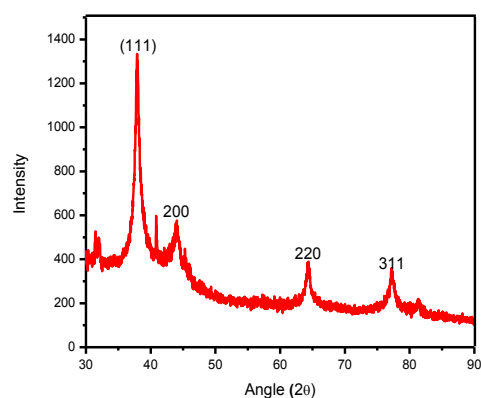
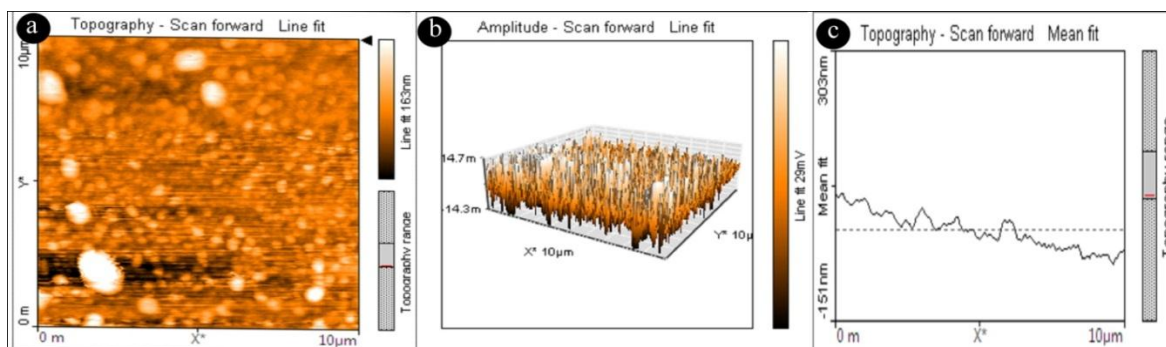


Fig. 4: X-ray Diffraction pattern of ZnNPs

### AFM and HR-TEM analysis

The morphology and size of zinc nanoparticles as revealed by AFM and HR-TEM found to be distinct nanostructures. The particles are monodispersed and spherical in shape with size range between 15 and 85 nm (Fig. 5a and Fig. 6).

The two and three dimensional view of sample represents structure of the nanoparticles with a height of 12.4 nm (Fig. 5b). The distance between from each other nanoparticle is 16.3 to 48.5 nm (Fig. 5c).



**Fig. 5: Atomic force microscopy images of ZnNPs synthesized by leaf extract of *G. floribunda* a) 2D image b) 3D image c) particle distribution of ZnNPs**

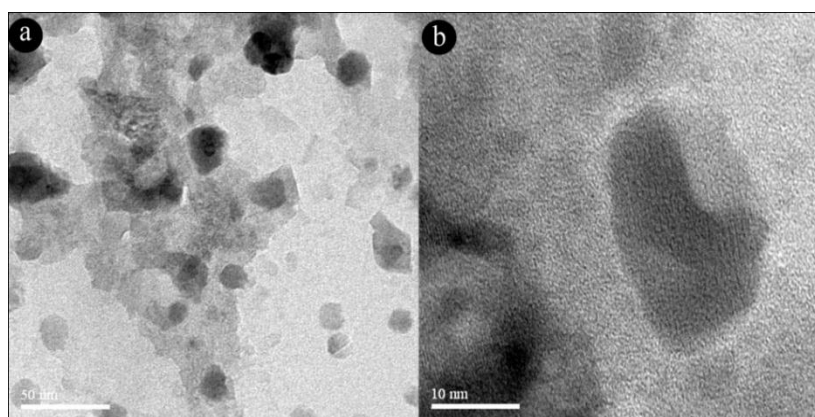


**Fig. 6: HR-TEM images of biosynthesized ZnNPs synthesized by leaf extract of *G. floribunda* a) 50 nm image b) 10 nm image of HR-TEM**

### Effect of ZnNPs on mitotic chromosomes of *D. polyantha*

The present investigation was undertaken to determine the effect of biogenic zinc nanoparticles synthesized by leaf extract of *G. floribunda* on root tip meristematic cells of *D. polyantha*. *D. polyantha* is a wild bulbous plant used for cytotoxic and genotoxic assay. The root tip cells were treated with viz. 4, 8, 12 and 16 μg/ml concentrations of ZnNPs solution for 6, 12, 18 and 24 hrs. The results revealed that the mitotic index values found to be decreased with increasing concentrations of zinc nanoparticles up to 16 μg/ml for 24 hrs exposure duration, when compared to control (Table 2 and Figure 7). Statistically, the data found to be significant at ( $p < 0.05$ ). The decrease in mitotic index was dose and duration dependent in root tip cells of *D. polyantha*. Coelcho et al.<sup>28</sup> suggested that a reduction in the number of dividing cells is an

evidence of mitodispersive effect of ZnNPs on cell division, which cause inhibition of DNA synthesis or blocking G2 phase to prevent the cell from entering mitosis<sup>29-30</sup>. This is similar to previous studies wherein the aqueous extract of different medicinal plants caused inhibition of mitotic cell division in *Allium cepa* root tips<sup>31-35</sup>. The tiny sized nanoparticles have greater tendency to enter subcellular organelles and may interact directly or indirectly with the genetic material (DNA) via nuclear pores causing clastogenic effects on cell cycle leading to DNA damage and formation of micronucleus was apparent through oxidative stress<sup>36-37</sup>. Similar results have been reported by several workers by using different plant model systems such as *Zea mays*, *Nigella sativa*, *Triticum aestivum*, *Allium cepa*, *Vicia faba*, and *Drimia indica* which support our studies<sup>38,39,10,40,17,12</sup>.

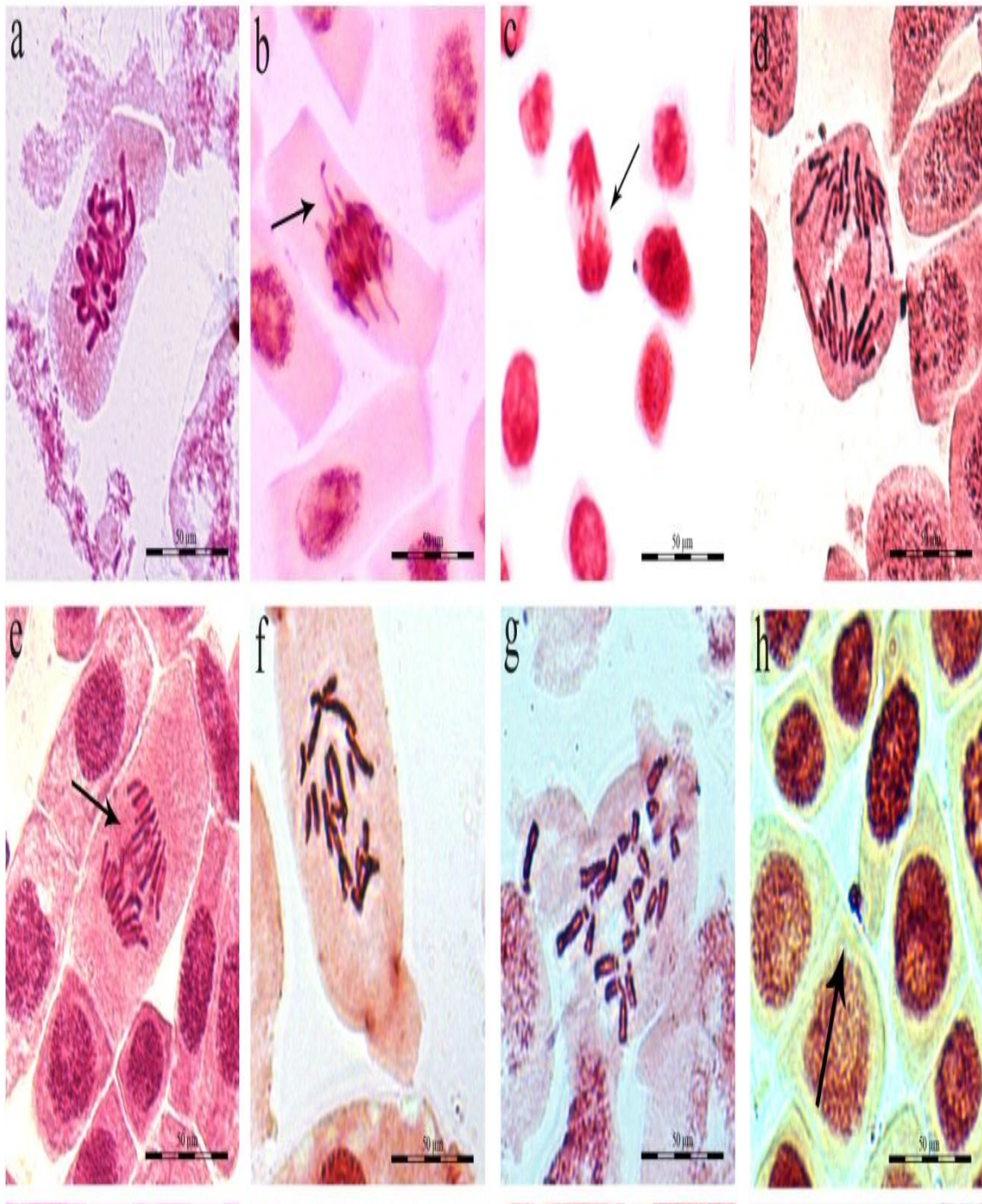


**Fig. 7: Chromosomal abnormalities observed in root tip meristematic cells of *D. polyantha* exposed to different concentrations of ZnNPs. a) sticky metaphase b) laggard at metaphase c) single bridge at anaphase d) multipolar anaphase e) multibrIDGE at anaphase f) spindle disturbance at anaphase g) C-metaphase h) micronucleus**

**Table 2: The effect of ZnNPs on mitotic index (MI) of root tip meristematic cells of *D. polyantha***

Duration (hrs)	Concentration ( $\mu\text{g/ml}$ )	Total No. of cells examined	No. of dividing cells	No. of non dividing cells	P%	M%	A%	T%	MI%
	Control	2417	1413	1004	92.74 $\pm$ 2.05	2.89 $\pm$ 0.76	2.56 $\pm$ 0.70	1.77 $\pm$ 0.07	58.25 $\pm$ 7.08
6	4	2184	1130	1054	94.28 $\pm$ 1.49	2.84 $\pm$ 1.01	1.72 $\pm$ 0.07	0.42 $\pm$ 0.01	51.71 $\pm$ 5.47
	8	2158	1044	1114	93.49 $\pm$ 1.44	3.39 $\pm$ 0.73	1.36 $\pm$ 0.09	0.39 $\pm$ 0.02	48.43 $\pm$ 2.68
	12	2246	1048	1198	92.30 $\pm$ 1.04	3.70 $\pm$ 0.20	1.52 $\pm$ 0.06	0.39 $\pm$ 0.02	46.63 $\pm$ 3.12
	16	2204	1003	1201	90.72 $\pm$ 1.64	4.90 $\pm$ 0.77	1.09 $\pm$ 0.04	0.69 $\pm$ 0.01	45.54 $\pm$ 2.58
12	4	2093	926	1167	90.47 $\pm$ 0.82	3.90 $\pm$ 1.07	1.82 $\pm$ 0.01	0.53 $\pm$ 0.01	44.23 $\pm$ 1.22
	8	2207	975	1232	89.62 $\pm$ 1.33	4.93 $\pm$ 0.44	1.54 $\pm$ 0.03	0.50 $\pm$ 0.06	44.15 $\pm$ 1.11
	12	2160	911	1249	87.45 $\pm$ 2.40	5.46 $\pm$ 0.57	1.99 $\pm$ 0.07	0.54 $\pm$ 0.09	42.15 $\pm$ 0.99
	16	2202	930	1272	87.40 $\pm$ 0.64	5.28 $\pm$ 1.27	2.58 $\pm$ 0.85	0.62 $\pm$ 0.06	42.18 $\pm$ 1.28
18	4	1915	709	1206	84.36 $\pm$ 3.04	4.67 $\pm$ 1.18	3.40 $\pm$ 0.06	0.69 $\pm$ 0.02	37.01 $\pm$ 0.87
	8	2080	745	1335	82.43 $\pm$ 4.10	5.63 $\pm$ 0.36	3.08 $\pm$ 0.52	0.53 $\pm$ 0.04	35.81 $\pm$ 0.42
	12	2115	690	1425	82.65 $\pm$ 3.40	5.04 $\pm$ 0.79	3.38 $\pm$ 0.48	0.84 $\pm$ 0.07	32.60 $\pm$ 1.43
	16	1935	655	1280	78.75 $\pm$ 1.91	5.65 $\pm$ 0.67	3.79 $\pm$ 0.82	1.04 $\pm$ 0.06	34.01 $\pm$ 3.79
24	4	1992	543	1449	73.04 $\pm$ 3.73	4.64 $\pm$ 0.57	2.65 $\pm$ 0.15	1.12 $\pm$ 0.05	27.24 $\pm$ 3.20
	8	1813	477	1336	68.32 $\pm$ 3.17	4.84 $\pm$ 0.90	2.73 $\pm$ 0.05	1.67 $\pm$ 0.03	26.39 $\pm$ 2.45
	12	1861	412	1449	59.69 $\pm$ 1.16	4.68 $\pm$ 0.52	2.88 $\pm$ 0.56	1.98 $\pm$ 0.03	22.09 $\pm$ 0.32
	16	1748	341	1407	49.20 $\pm$ 1.35	3.50 $\pm$ 0.63	1.71 $\pm$ 0.07	2.65 $\pm$ 0.08	19.43 $\pm$ 1.58

Where, P- prophase; M-metaphase; A-anaphase; T-telophase; MI- mitotic index  
Statically significant at  $p < 0.05$ , analyzed by Two-way ANOVA (Tukey test)

In another study, genotoxic effect can be analyzed by observing chromosomal abnormalities. Chromosomal aberrations are structural changes in chromosomes or chromatid breaks resulting dicentric chromosomes. There were no chromosomal aberrations were observed in the control. The maximum proportion of chromosomal aberrations was recorded in 16  $\mu\text{g/ml}$  of ZnNPs suspension (14.79 $\pm$ 12.27%) for 24 hrs of exposure duration. The results were statistically significant at ( $p < 0.05$ ), when compared to control. The observed chromosomal aberrations induced may be due to the presence of some naturally occurring phytochemical compounds in the leaf extract such as terpenoids, sterols, alkaloids and flavanoids<sup>18</sup> have been implicated in chromosomal damage at higher concentrations<sup>41-44</sup>. When these higher concentrations of ZnNPs enter into the root tip cells, changes the chromosomal behavior such as bridges, sticky, laggard, diagonal, C-metaphase, multipolar anaphase, disturbed metaphase and micronucleus (Table 3 and Fig. 7).

The occurrence of various forms of chromosomal aberrations was detected in all phases of mitosis. The chromosomes appear sticky due to physiological stress as a result of asphyxiation. Extreme treatment conditions for prolonged duration cause cellular asphyxiation causing respiratory inhibition leading to cell death. The chromosome stickiness and spindle malfunction was evident in the absence of cellular energy ATP. In addition, laggard chromosomes are formed by the failure of spindle fiber or acentric chromosome formation. The occurrence of C- metaphase indicates the risk of aneuploidy, causing partial disturbance in the spindle apparatus<sup>45</sup>. Chromosomal bridges were also frequent in ZnNPs suspension, which occur in anaphase-telophase stages of mitosis. Bridges may occur during the translocation of unequal sister chromatid exchange and cause structural chromosome mutation<sup>32, 34</sup>. The Lagging chromosomes are formed by separation of daughter nuclei with unequal number of chromosomes and subsequent formation of micro nuclei or daughter cells with unequal sizes at intervals.

**Table 3: Chromosomal aberrations observed in root tip meristematic cells of *D. polyantha***

Duration (hrs)	Concentration ( $\mu\text{g/ml}$ )	CB	Sticky	laggard	Multipolar	lagging	Micro	MB	C-meta	CAs (%)
	Control	0.00 $\pm$ 0.00	0.00 $\pm$ 0.00	0.00 $\pm$ 0.00	0.00 $\pm$ 0.00	0.00 $\pm$ 0.00	0.00 $\pm$ 0.00	0.00 $\pm$ 0.00	0.00 $\pm$ 0.00	0.00 $\pm$ 0.00
6	4	0.10 $\pm$ 0.07	0.26 $\pm$ 0.04	0.80 $\pm$ 0.03	0.87 $\pm$ 0.05	0.81 $\pm$ 0.02	0.00 $\pm$ 0.00	0.00 $\pm$ 0.00	0.00 $\pm$ 0.00	0.69 $\pm$ 0.06
	8	0.17 $\pm$ 0.03	0.64 $\pm$ 0.06	0.20 $\pm$ 0.05	0.10 $\pm$ 0.07	0.10 $\pm$ 0.05	0.00 $\pm$ 0.00	0.00 $\pm$ 0.00	0.00 $\pm$ 0.00	1.34 $\pm$ 0.07
	12	0.30 $\pm$ 0.01	0.79 $\pm$ 0.08	0.40 $\pm$ 0.08	0.18 $\pm$ 0.05	0.18 $\pm$ 0.03	0.00 $\pm$ 0.00	0.00 $\pm$ 0.00	0.90 $\pm$ 0.05	2.05 $\pm$ 0.05
	16	0.39 $\pm$ 0.03	1.57 $\pm$ 0.09	0.00 $\pm$ 0.00	0.00 $\pm$ 0.00	0.20 $\pm$ 0.04	0.10 $\pm$ 0.07	0.00 $\pm$ 0.00	0.20 $\pm$ 0.04	2.57 $\pm$ 0.06
12	4	0.11 $\pm$ 0.09	1.17 $\pm$ 0.01	0.77 $\pm$ 0.09	0.22 $\pm$ 0.03	0.20 $\pm$ 0.07	0.20 $\pm$ 0.05	0.11 $\pm$ 0.09	0.19 $\pm$ 0.03	3.24 $\pm$ 0.08
	8	0.30 $\pm$ 0.09	1.33 $\pm$ 0.01	0.50 $\pm$ 0.07	0.31 $\pm$ 0.02	0.20 $\pm$ 0.05	0.10 $\pm$ 0.01	0.00 $\pm$ 0.00	0.10 $\pm$ 0.07	3.38 $\pm$ 0.08
	12	0.55 $\pm$ 0.01	1.53 $\pm$ 0.05	0.98 $\pm$ 0.01	0.44 $\pm$ 0.08	0.23 $\pm$ 0.09	0.00 $\pm$ 0.00	0.10 $\pm$ 0.05	0.11 $\pm$ 0.09	4.51 $\pm$ 0.43
	16	0.90 $\pm$ 0.06	1.66 $\pm$ 0.08	0.00 $\pm$ 0.00	0.34 $\pm$ 0.05	0.35 $\pm$ 0.06	0.31 $\pm$ 0.09	0.96 $\pm$ 0.07	0.35 $\pm$ 0.05	4.80 $\pm$ 0.09
18	4	0.28 $\pm$ 0.04	2.17 $\pm$ 0.09	1.13 $\pm$ 0.25	0.68 $\pm$ 0.04	0.69 $\pm$ 0.02	0.25 $\pm$ 0.04	0.30 $\pm$ 0.05	0.38 $\pm$ 0.06	6.84 $\pm$ 0.55
	8	0.52 $\pm$ 0.04	2.01 $\pm$ 0.07	1.21 $\pm$ 0.05	0.93 $\pm$ 0.05	0.00 $\pm$ 0.00	0.52 $\pm$ 0.09	0.26 $\pm$ 0.02	0.65 $\pm$ 0.08	8.29 $\pm$ 0.65
	12	0.57 $\pm$ 0.07	2.52 $\pm$ 0.51	1.59 $\pm$ 0.06	0.29 $\pm$ 0.05	0.69 $\pm$ 0.08	0.29 $\pm$ 0.05	0.00 $\pm$ 0.00	0.29 $\pm$ 0.05	8.04 $\pm$ 0.26
	16	0.46 $\pm$ 0.05	2.30 $\pm$ 0.57	1.39 $\pm$ 0.04	1.67 $\pm$ 0.08	0.78 $\pm$ 0.03	0.44 $\pm$ 0.05	0.57 $\pm$ 0.06	0.63 $\pm$ 0.04	10.73 $\pm$ 1.52
24	4	0.50 $\pm$ 0.05	5.16 $\pm$ 2.26	2.30 $\pm$ 0.17	1.37 $\pm$ 0.19	1.23 $\pm$ 0.07	0.67 $\pm$ 0.06	0.33 $\pm$ 0.07	0.50 $\pm$ 0.08	14.36 $\pm$ 2.47
	8	1.27 $\pm$ 0.08	6.01 $\pm$ 2.27	3.41 $\pm$ 0.04	1.25 $\pm$ 0.07	2.06 $\pm$ 0.24	0.42 $\pm$ 0.07	0.42 $\pm$ 0.02	0.84 $\pm$ 0.07	18.45 $\pm$ 1.27
	12	1.86 $\pm$ 0.04	6.46 $\pm$ 0.13	3.26 $\pm$ 0.90	2.56 $\pm$ 0.51	2.72 $\pm$ 0.34	0.84 $\pm$ 0.06	1.34 $\pm$ 0.03	1.65 $\pm$ 0.05	23.24 $\pm$ 3.20
	16	2.93 $\pm$ 0.34	10.55 $\pm$ 0.95	4.88 $\pm$ 0.59	4.57 $\pm$ 0.83	3.47 $\pm$ 0.50	1.50 $\pm$ 0.06	2.37 $\pm$ 0.05	1.78 $\pm$ 0.08	36.09 $\pm$ 3.29

Where, CB- chromosomal bridge; MB-multibridge at anaphase; CAs- chromosomal aberrations Statically significant at  $p < 0.05$ , analyzed by Two-way ANOVA (Tukey test)

Earlier reports revealed that *Allium cepa* root tip cells have been widely applied to evaluate cytotoxicity and genotoxicity induced by pesticides<sup>46</sup>, herbicides<sup>47</sup>, Aromatic hydrocarbons<sup>48-49</sup>, Textile industry dyes<sup>29, 50</sup>, heavy metals<sup>51</sup> and higher plants<sup>52, 10</sup> showed positive results by using these parameters for the analysis of chromosomal abnormalities and also showing a greater genotoxic effect on root tip cells. The results of present investigation suggest that biogenic zinc nanoparticles inhibit cell division at higher concentrations was found to be strongly concentration and duration dependent. The induction of chromosomal aberrations observed in the root tip cells of *D. polyantha*, was due to the bio-uptake nanoparticles from the suspensions.

### CONCLUSION

In the present study zinc nanoparticles synthesized by *G. floribunda* leaf extract, showed higher cytotoxic and genotoxic activity using root tip meristematic cells of *D. polyantha*. The toxicity is found to be concentration and duration dependent and decrease in mitotic

index and increase in chromosomal aberrations confirming the cytotoxic and genotoxic level of zinc nanoparticles.

### ACKNOWLEDGEMENTS

The authors are thankful to the Chairman, P. G. Department of Studies in Botany, Karnatak University, Dharwad, for providing the necessary facility and UGC-DSA-I phase of Department for financial assistance. One of the author (A.D) acknowledges the Directorate of Minorities, Government of Karnataka, for awarding Research fellowship. The Authors also thank USIC- KUD, MIT Manipal and IITM Chennai for instrumentation facility.

### REFERENCES

1. Meulenkamp EA. Synthesis and growth of ZnO nanoparticles. J Phys Chem B. 1998;102:5566-5572.
2. Serpone N, Dondi D and Albini A. Inorganic and organic UV filters: their role and efficacy in sunscreens and sun care product. Inorg Chim Acta. 2007;360:794-802.

3. Kathiresan K, Manivannan S, Nabeel MA and Dhivya B. Studies on silver nanoparticles synthesized by a marine fungus, *Penicillium fellutanum* isolated from coastal mangrove sediment, *Colloids Surf B*. 2009;71(1):133–137.
4. Qi WH and Wang MP. Size and shape dependent melting temperature of metallic nanoparticles, *Mater Chem Phys*. 2004;88:280–284.
5. Roduner E. Size matters: why nanomaterials are different. *Chem Soc Rev*. 2006;35(7):583–592.
6. Keat CL, Azila AA, Eid AM and Elmarzugi NA. Biosynthesis of nanoparticles and silver nanoparticles, *Bioresour. Bioprocess*. 2015; 2:47.
7. Mohanpuria P, Rana N and Yadav S. Biosynthesis of nanoparticles: technological concepts and future applications. *J Nanopart Res*. 2008;10(3):507–517.
8. Iravani S. Green synthesis of metal nanoparticles using plants. *Green Chem*. 2011;13(10):2638–2650.
9. Prabhu S and Poulouse E. Silver nanoparticles: mechanism of antimicrobial action, synthesis, medical applications and toxicity effects. *Int Nano Lett*. 2012;2(1):1-10.
10. Taranath TC, Bheemanagouda NP, Santosh TU and Sharath BS. Cytotoxicity of zinc nanoparticles fabricated by *Justicia adhatoda* L. on root tips of *Allium cepa* L. A model approach. *Environ Sci Pollut Res*. 2015;22:8611–8617.
11. Bheemanagouda NP and Taranath TC. *Limonia acidissima* L. leaf mediated synthesis of zinc oxide nanoparticles: A potent tool against *Mycobacterium tuberculosis*. *International Journal of Mycobacteriology*. 2016;5:197-204.
12. Azharuddin D, Taranath TC. Biosynthesis of silver nanoparticles by leaf extract of *Albizia saman* (Jacq.) Merr. and their cytotoxic effect on mitotic chromosomes of *Drimia indica* (Roxb.) Jessop. *Environ Sci Pollut Res*. 2017:1-9.
13. Lin D and Xing B. Root uptake and phytotoxicity of ZnO nanoparticles. *Environ Sci Technol*. 2008;42:5580–5585.
14. Lee CW, Mahendra S, Zodrow K, Li D, Tsai YC and Braam J. Developmental phytotoxicity of metal oxide nanoparticles to *Arabidopsis thaliana*. *Environ Toxicol Chem*. 2010;29:669-675.
15. Fukui H, Horie M, Endoh S, Kato H, Fujita K, Nishio K, Komaba LK, Maru J, Miyauhi A, Nakamura A, Kinugasa S, Yoshida Y, Hagihara Y and Iwahashi H. Association of zinc ion release and oxidative stress induced by intratracheal instillation of ZnO nanoparticles to rat lung. *Chem Biol Interact*. 2012;198(1):29–37.
16. Eshed M, Lellouche J, Matalon S, Gedanken A and Banin E. Sonochemical coatings of ZnO and CuO nanoparticles inhibit *Streptococcus mutans* biofilm formation on teeth model. *Langmuir*. 2012;28:12288–12295.
17. Ahmed B, Dwivedi S, Abdin MZ, Azam A, Al-Shaeri M, Khan MS, Saquib Q, Al-Khedhairy AA, Musarrat J, Mitochondrial and chromosomal damage induced by oxidative stress in Zn<sup>2+</sup> ions, ZnO-bulk and ZnO-NPs treated *Allium cepa* roots, *Scientific reports*. 2016;7:40685.
18. Glory A, Judin J, Vasudevan R and Sumathi P. Preliminary phytochemical content and antibacterial activity of *Ukshi* (*Calycopteris floribunda* Lam.) leaves. *Journal of Medicinal Plants Studies*. 2016;4(2):57-59.
19. Dey SK, Shoeb Mohammed, Rob Tamanna, Nilafar Nahar, Mosihuzzaman M and Nasin Sultana. Biological and chemical studies of *Calycopteris floribunda* leaves. *The Dhaka Univ. J Pharm Sci*. 2005;4(2):1816-1839.
20. Bhat PR, Prajna PS, Kumar V, Hegde AM and Singh L. Antimicrobial properties of leaves of *Calycopteris floribunda* Lam. *Journal of Medicinal Plants Research*. 2011;5(12):2448-2451.
21. Sharma AK. *Chromosome Technique Theory and Practice*, 3<sup>rd</sup> ed. Butterworth, London, 1980.
22. Fiskesjo G. Allium test on river water from Braan and Saxan before and after closure of a chemical factory, *Ambio*. 1985;14:99–103.
23. Fiskesjo G. Allium test for screening chemicals; evaluation of cytologic parameters, in Wang W, Gorsuch JW and Hughes JS. (Eds.). *Plants for Environmental Studies*, CRC Lewis Publishers, Boca Raton NY. 1997;308–333.
24. Ozmen A and Celik TA. Cytotoxic effects of peel extracts from *Citrus limon* and *Citrus sinensis*. *Caryologia*. 2007;60(1-2):48-51.

25. Narendhran S and Sivaraj R. Biogenic ZnO nanoparticles synthesized using *L. aculeata* leaf extract and their antifungal activity against plant fungal pathogens. *Bull Mater Sci.* 2016;39(1): 1-5.
26. Geethalakshmi R, Sakravarthi C, Kritika T, Arul Kirubakaran M and Sarada DVL. Evaluation of Antioxidant and Wound Healing Potentials of *Sphaeranthus amaranthoides* Burm.f. *BioMed Research International.* 2013;7:607109.
27. Gopinath K, Gowri S, Karthika V and Arumugam A. Green synthesis of gold nanoparticles from fruit extract of *Terminalia arjuna*, for the enhanced seed germination activity of *Gloriosa superba*. *J Nanostruct Chem.* 2014;4:115.
28. Coelho APD, Laughinghouse HD, Kuhn AW, Boligon AA, do Canto-Dorow TS, Ferreira da Silva AC and Tedesco SB. Genotoxic and antiproliferative potential of extracts of *Echinodorus grandiflorus* and *Sagittaria montevidensis* (Alismataceae). *Caryologia.* 2017;70(1):82-91.
29. Sudhakar R, Ninge Gowda KN and Venu G. Mitotic abnormalities induced by silk dyeing industry effluents in the cells of *Allium cepa*. *Cytologia.* 2001;66:235-239.
30. Karaismailoglu MC. Investigation of the potential toxic effects of prometryne herbicide on *Allium cepa* root tip cells with mitotic activity, chromosome aberration, micronucleus frequency, and nuclear DNA amount and comet assay. 2016:2165-5391.
31. Frescura VD, Kuhn AW, Laughinghouse IVHD, Nicoloso FT, Lopes SJ and Tedesco SB. Evaluation of the allelopathic, genotoxic, and antiproliferative effect of the medicinal species *Psychotria brachypoda* and *Psychotria birotula* (Rubiaceae) on the germination and cell division of *Eruca sativa* (Brassicaceae). *Caryologia.* 2013;66:138-144.
32. Khanna N and Sharma S. *Allium cepa* root chromosomal aberration assay: a review. *Indian Journal of Pharmaceutical and Biological Research.* 2013;1:105-119.
33. Lamsal K, Ghimire BK, Sharma P, Ghimiray AK, Kim SW, Yu CY, Chung IM, Lee YS, Kim J and Shakya SR. Genotoxicity evaluation of the insecticide ethion in root of *Allium cepa* L. *African Journal of Biotechnology.* 2010;9: 4204-4210.
34. Prajitha V and Thoppil JE. Genotoxic and antigenotoxic potential of the aqueous leaf extracts of *Amaranthus spinosus* Linn. using *Allium cepa* assay, *South African Journal of Botany.* 2016; 102:18-25.
35. Akinboro A and Bakare AA. Cytotoxic and genotoxic effects of aqueous extracts of five medicinal plants on *Allium cepa* Linn. *Journal of Ethnopharmacology.* 2007;112:470-475.
36. Boyoglu C, He Q, Willing G, Boyoglu-Barnum S, Vida AD, Pillai S and Singh SR. Microscopic studies of various sizes of gold nanoparticles and their cellular localizations. *ISRN Nanotechnol.* 2013; 123838: 13.
37. Magdolenova Z, Collins A, Kumar A, Dhawan A, Stone V and Dusinska M. Mechanisms of genotoxicity. A review of in vitro and in vivo studies with engineered nanoparticles. *Nanotoxicology.* 2014;8(3):233-78.
38. De Campos JMS and Viccini LF. Cytotoxicity of aluminum on meristematic cells of *Zea mays* and *Allium cepa*. *Caryologia.* 2003;56(1):65-73.
39. El-Ghamery AA, El-Kholy MA and Abou El-Yousser MA. Evaluation of cytological effects of Zn<sup>2+</sup> in relation to germination and root growth of *Nigella sativa* L. and *Triticum aestivum* L. *Mutation Research.* 2003;537:29-4.
40. Ruffini Castiglione M, Lucia G, Lorenza B, Simonetta M, Stefania B and Carmelina S. Root responses to different types of TiO<sub>2</sub> nanoparticles and bulk counterpart in plant model system *Vicia faba* L. *Environmental and Experimental Botany.* 2016;130.
41. Ene EE and Osuala CL. The mutagenic potentials of water extract of *Borreria filiformis* (Hiern) Hatch and Dalz. and *Vince rosea* Linn. *Nig J Bot.* 1990;3:35-40.
42. Yamanaka N, Oda O and Nagao S. Green tea catechins such as (-)-epicatechin and (-)-epigallocatechin accelerate Cu<sup>2+</sup> induced low density lipoprotein oxidation in propagation phase. *FEBS Letters.* 1997;401:230-234.
43. Hayakawa F, Kimura T, Hoshimo N and Ando T. DNA cleavage activities of (-) epigallocatechin, (-)-epicatechin, (+)-catechin, and (-)-epigallocatechin

- gallate with various kind of metal ions. *Biosci Biotechnol Biochem.* 1999;63:1654–1656.
44. Ifeoluwa TO and Bakare AA. Genotoxic and anti-genotoxic effect of aqueous extracts of *Spondias mombin* L., *Nymphaea lotus* L. and *Luffa cylindrica* L. on *Allium cepa* root tip cells. *Caryologia.* 2013; 66(4):360–367.
45. Pandey H, Kumar V and Roy BK. Assessment of genotoxicity of some common food preservatives using *Allium cepa* L. as a test plant, *Toxicology reports.* 2014;1:300-308.
46. Chauhan LKS, Saxena PN, Sundararaman V and Gupta SK. Diuron-induced cytological and ultrastructural alterations in the root meristem cells of *Allium cepa*. *Pest Biochem Physiol.* 1998;62:152-163.
47. Bolle P, Mastrangelo S, Tucci P and Evandri MG. Clastogenicity of atrazine assessed with the *Allium cepa* test. *Environ. Mol. Mutagen.* 2004;43:137-141.
48. Fiskesjo G and Lassen C. Benzo[a]pireno and nitrosoguanidine in the *Allium* test. *Mutat Res.* 1982;97:188.
49. Rank J and Nielsen MH. Evaluation of the *Allium* anaphase–telophase test in relation to genotoxicity screening of industrial wastewater. *Mutat Res.* 1994;312:17–24.
50. Carita R and Marin-Morales MA. Induction of chromosome aberrations in the *Allium cepa* test system caused by exposure of seeds to industrial effluents contaminated with azo dyes, *Chemosphere.* 2008;72:722–725.
51. Fiskesjo G. *Allium* test on copper in drinking water. *Vatten.* 1981;37:232–240.
52. Kumari M, Khan SS, Pakrashi S, Mukherjee A and Chandrasekaran N. Cytogenetic and genotoxic effects of zinc oxide nanoparticles on root cells of. *J Hazard Mater.* 2011;190(1–3):613–621.